Comparison of biophysical models with experimental data for three cell lines in response to irradiation with monoenergetic ions

Caterina Monini, Gersende Alphonse, Claire Rodriguez-Lafrasse, Etienne Testa, Michael Beuve

Comparison of biophysical models with experimental data for three cell lines in response to irradiation with monoenergetic ions

Caterina Monini [a *], Gersende Alphonse [a,b,c], Claire Rodriguez-Lafrasse [a,b,c], Étienne Testa [a] ,Michaël Beuve[a]

[a]Univ. Lyon, Univ. Claude Bernard Lyon 1, CNRS/IN2P3, IP2I Lyon, F-69622, Villeurbanne, France

[b]Laboratoire de Radiobiologie Cellulaire et Moléculaire, Faculté de Médecine Lyon-Sud

[c]Hospices Civils de Lyon, Service de Biochimie, Centre Hospitalier Lyon-Sud, 69495 Pierre-Bénite France

Corresponding author: Caterina Monini, monini@ipnl.in2p3.fr
Bâtiment Paul Dirac, Rue Enrico Fermi, 69622 Villeurbanne, France

Highlights:

- The accuracy of biophysical modeling is crucial for particle therapy
- Comparison of LEM(I-IV), MKM and NanOx models with data for 3 cell lines
- χ^2 scoring for α(LET) curves
- NanOx yields the highest score more often than the other models

Financial support**:**
ITMO Cancer in the framework of Plan Cancer 2009-2013 and Plan Cancer 2016-2019 (Project Nos. PC201312 and PC201606) referred to as: “Domaine de la physique, des mathématiques ou des sciences de l’ingénieur appliqués au Cancer”.

ABSTRACT

The relative biological effectiveness (RBE) in particle therapy is currently estimated using biophysical models. We compared experimental measurements to the α(LET) curves computed by the Local Effect Model (LEM I-IV), the Microdosimetric Kinetic Model (MKM) and the NanOx model for HSG, V79 and CHO-K1 cells in response to monoenergetic irradiations. Although the LEM IV and the MKM predictions accurately reproduced the trend observed in the data, NanOx yielded a better agreement than the other models for more irradiation configurations. Its χ^2 estimator was indeed the lowest for 3 over 7 considered cases.

1. INTRODUCTION

Due to its increased efficiency in inducing biological damage, particle therapy offers advantages over the standard radiotherapy modalities for the treatment of radioresistant, unresectable tumors close to organs at risk [1, 2]. Several experimental studies have shown evidence that the relative biological effectiveness (RBE) of ions with respect to photons depends on multiple parameters related to the incident beam, the irradiation conditions and the intrinsic properties of the biological system [2]. Therefore, to optimize the 3-dimensional distribution of the dose to be received by the patient during a session, the predictions of RBE are integrated into the treatment planning system (TPS). While the first approach used in clinics was based on RBE values derived empirically from the *in-vitro* response of a well-known tumor cell line to neutron beams [3], the progressive diffusion of active beam delivery favored the implementation of biophysical models in the TPS. This triggered the development and the improvement of many frameworks, the most acknowledged ones being the Local Effect Model (LEM) and the Microdosimetric Kinetic Model (MKM).

The LEM I [4, 5], II [6], III [7] ascribes the biological effectiveness of ions to the specific energy deposition pattern at "local" scale, which is estimated in terms of a radial dose (D(r)). Although enabling fast and efficient calculations, the use of the expected quantity D(r) to describe processes occurring at the nanoscale leads to some incongruities; for example, the shoulder in cell survival curves results from an artifact due to the superimposition of the radial doses associated to several impacting ions [14]. The issue was solved in the LEM IV [8], a substantially different version of the local effect model in which the cell nucleus is divided into critical regions corresponding to DNA giant loops. In these domains the microscopic spatial distribution of DNA double strand breaks is computed on the basis of the radial dose.

The MKM [9] combines a microdosimetric description of the energy deposition (accounting for the statistical fluctuations) with a kinetic representation of the repair and injury processes. The probability of cell survival, however, is not computed considering an average process over the irradiation configurations, but simply in terms of a Poisson distribution of the mean number of lethal lesions. The distribution is corrected defining a geometry for the cell nucleus in order to avoid the overestimation of the ions efficacy in the tumor [10].

More recently, NanOx [11, 12, 13] was developed by the authors to address the challenge of implementing the stochasticity of the energy depositions at nanometric and microscopic scales when predicting radiation-induced effects. This is fulfilled in the modeling of the number of radiation impacts associated to a given dose, of the dose-deposition pattern along the track and of the inter-track processes. The cell inactivation is ascribed to two classes of biological events occurring at different spatial and temporal scales, in a manner similar to that proposed by Katz *et al.* [15]. Local lethal events are attributed to one track and are described in terms of nanodosimetry, while global events resulting from the contribution of several tracks are represented by the accumulation of oxidative stress and sublethal damages.

We decided to benchmark the predictions issued from these models against experimental data to verify if the implementation of a fully stochastic theory at nano and micro-scale had an impact on the precision of the predictions. In this paper we considered as biological endpoint the slope of cell survival curves since this is the one reported most extensively in the literature, both for measurements and theoretical calculations.

2. MATERIALS AND METHODS

2.1 Experimental data

Our study focused on the response of three cell lines to monoenergetic beams of several ion types (from hydrogen to neon) and energies (from 0.8 to 266 MeV/n).We chose normal lung fibroblast (V79) and ovary (CHO-K1) cells from a Chinese hamster due to the large amount of data available in the literature, and human tumor cells from salivary glands (HSG) since head and neck cancers match the therapeutic indications for particle therapy.

The experimental α values were gathered from the database made available by the PIDE project [17]. Although for most of the measurements the error bars are not reported, the great data dispersion allows one to infer the important biological

variability and the effects of the use of different biological and irradiation protocols. In spite of this dispersion, however, it is noticeable that α values rise for LET values up to 150-200 keV/μm (depending on the ion type), and drop for higher LET values. The initial trend is associated to the action of swift ions, which scarcely ionize the traversed biological tissues by depositing only small amounts of energy; progressively slower ions, on the contrary, produce a considerable ionization density in the medium leading to the increase of the biological effectiveness. The decrease of the α curves is due to the "overkill" effect, which may be explained in terms of two phenomena: firstly, for constant irradiation doses the fluence of incident particles is inversely proportional to the LET, and secondly, the tracks of high LET ions are narrow; the probability of hitting the cellular sensitive targets and inducing biological damages is, thus, fairly low.

2.2 Models predictions

The α values predicted by the LEM I, II, III, IV and the MKM for all the considered radiation types and cell lines were extracted from [8, 16] and for each of these models, the calculations were reported only for the irradiation cases for which published results could be found. The values of α predicted by NanOx, on the contrary, were computed by the authors especially for this work. Precisely, theoretical cell survival curves were first calculated as explained in [11, 13], and then a linear fit at low doses allowed extraction of the slope α.

As Table 1 shows, all the models were evaluated considering a unique set of parameters per cell line, *i.e.* avoiding tuning and optimizations which would depend on the irradiation ion type. As explained in [8, 12, 16], the choice of the parameters was made in order to optimize the conformity between the predicted α values and the experimental ones available from the literature.

2.3 Benchmark estimator

In order to quantify the agreement between the predictions issued from each model and the data, we computed the χ^2 as:

$$\chi^2 = \frac{1}{M}\sum_{i=1}^{M}\left(\frac{\alpha_{exp}^{i}-\alpha_{pred}^{i}}{\alpha_{exp}^{i}}\right)^2 \qquad (1)$$

In Eq. 2, M represents the total number of experimental points pertaining to the PIDE dataset [17] for a given cell line and ion type, and α_{exp}^{i} (respectively α_{pred}^{i}) denotes the i^{th} experimental (resp. predicted) α value.

3. RESULTS

Figure 1 shows the slope α as a function of LET for HSG, V79 and CHO-K1 cells in response to hydrogen, helium, carbon, oxygen and neon ions. While the LEM I was inadequate to reproduce the experimental trend for almost all of the considered cell lines and radiation types, some amelioration was visible for the LEM II and III, mostly in the high LET range. An important disagreement between theoretical and observed α values, however, was apparent in the low LET range: the curves predicted by the LEM II (except for CHO-K1 cells in response to carbon ions) and by the LEM III in the case of irradiation by light ions, were overestimated, whilst the curves predicted by the LEM III for heavy ions irradiation, on the contrary, were underestimated. On the other hand, the experimental increase of α for LET values up to 150-200 keV/μm and the subsequent decrease observed for higher LET were overall well reproduced by the MKM, the LEM IV and the NanOx model. **Figure 2** and **Table 2** present the χ^2 estimator for each model, cell line and ion type. The intercomparison highlighted that NanOx's predictions were the most precise over the seven configurations, yielding the minimum χ^2 in three cases: for HSG cells in response to He ions, for V79 cells in response to C ions and for CHO-K1 cells in response to C ions. Our model was followed by the LEM IV and the MKM, which achieved the smallest χ^2 in two cases each.

DISCUSSION

The optimization of treatment plans in particle therapy strongly relies on the link between the energy deposition pattern and the expected biological response. Since such a link is currently provided by the biophysical model specifically implemented, it is of utmost importance to review and compare the main existing frameworks.

Recently, Stewart *et al.* [18] pointed out the differences among the LEM IV, the MKM and the Repair-Misrepair-Fixation (RMF) model in the input parameters, the relevant biological targets and the computational strategies. The main principles and the seemingly contradictory aspects of the models were discussed, but the article did not report an extensive benchmark of the different predictions against radiobiological measurements. Stewart *et al.* concluded that "future comparisons of model predictions with experimental data are needed to fully discriminate among competing mechanisms and models of particles RBE". We hence decided to test the accuracy of well-known cell survival models

considering a common biological endpoint, the α(LET) curves of HSG, V79 and CHO-K1 cells in response to monoenergetic irradiations, and as well as to examine the predictive power of NanOx. In order to quantify the agreement of the predictions with the experimental measurements found in the literature, a χ^2 calculation was performed for each cell line and irradiation type: NanOx yielded the lowest χ^2 for more configurations than the other models. This result should be considered in light of two facts: first, in some cases the difference in the χ^2 was small; and second, according to the published references several calculations were missing for the seven irradiation configurations that we considered. In particular, since the LEM IV predictions were available for only 3 cases, this model achieved the highest percentage of lowest χ^2 values. More generally, our study highlighted that the predictions issued by the LEM IV, the MKM and the NanOx model were appropriate considering the important dispersion of the experimental data, while the LEM I, II and III did not satisfactorily reproduce the observed biological effect of ions.

Even though the irradiation of *in-vitro* cells considered in our study are by far not representative of particle therapy treatments, a question may arise on the relevance of the current implementation of biophysical models in the clinical TPS.

The LEM I represents the standard in the European particle therapy facilities since it minimizes the risk of overestimating the doses prescribed to patients, and complies with the need of radiotherapists to rely on stable protocols. However, its description of the radiobiological response of V79, CHO-K1 and HSG cells was the least accurate among the models considered in our study. A modified version of the MKM (mMKM [21, 22, 23]) developed by Kase *et al.* is instead integrated in the Japanese clinical TPS. It predicts the decrease of RBE caused by the overkill effect owing to a revised saturation correction, and is based on amorphous track structure models (i.e. on the controversial radial dose), allowing fast calculations. We believe that in the context of clinical research it would be relevant to evaluate the predictive qualities of other biophysical models and of the several modified and improved versions of the existing frameworks. This could be achieved, for example, by performing calculations with each model in clinical conditions and trying to correlate them to clinical data; it would be fruitful to bridge over the advances in research and the clinical routine of particle therapy.

In conclusion, we showed in this paper that NanOx predictions for three cell lines irradiated by monoenergetic ions were more often more accurate than the ones issued from 5 other biophysical models; however, in some cases the difference with respect to the LEM IV and the MKM was small, and some theoretical calculations were missing. More reliable conclusions may be derived if an experimental dataset characterized by lower biological variability was available, and if all the biophysical models were tested more systematically for a wide range of irradiation configurations.

ACKNOWLEDGMENTS

This work was supported by ITMO Cancer (Project Nos. PC201312 and PC201606) and was performed in the framework of the LABEX PRIMES (ANR-11-LABX-0063) within the program "Investissements d'Avenir" (ANR-11-IDEX-0007) operated by the French National Research Agency. We thank Jayde Livingstone for her careful reading.

DECLARATION

The authors declare no conflicts of interest.

REFERENCES

1. Durante M, Orecchia R, Loeffler JS. Charged-particle therapy in cancer: clinical uses and future perspectives. Nat. Rev. Clin. Oncol. 2017; 14: 483-495.
2. Karger CP, Peschke P. RBE and related modeling in carbon-ion therapy. Phys. Med. Biol. 2017; 63: 01TR02.
3. Hirao Y, Ogawa H, Yamada S, Sato Y, Yamada T, Sato K et al.Heavy ion synchrotron for medical use –HIMAC project at NIRS, Japan. Nucl. Phys. A 1992; 538: 541-550.
4. Scholz M, Kellerer A, Kraft-Weyrather W, Kraft G. Computation of cell survival in heavy ion beams for therapy. The model and its approximation. Radiat. Environ. Biophys. 1997; 36: 59-66.
5. Kramer M, Jakel O, Harberer T, Kraft G, Schardt D, Weber U. Treatment planning for heavy-ion radiotherapy: physical beam model and dose optimization. Phys. Med. Biol. 2000; 45: 3299-3317.
6. Elsässer T and Scholz M. Cluster effects within the local effect model. Radiat. Res. 2007; 167: 319-329.
7. Elsässer T, Krämer M, Scholz M. Accuracy of the local effect model for the prediction of biologic effects of carbon ion beams in vitro and in vivo. Int. J. Radiat. Oncol. Biol. Phys. 2008; 71: 866-872.

8. Elsasser T, Weyrather W, Friedrich T, Durante M, Iancu G, Krämer M et al. Quantification of the relative biological effectiveness for ion beam radiotherapy: direct experimental comparison of proton and carbon ion beams and a novel approach for treatment planning. Int. J. Radiation Oncology Biol. Phys. 2010; 78: 1177-1183.

9. Hawkins RB. A microdosimetric-kinetic model of cell death from exposure to ionizing radiation of any let, with experimental and clinical applications. Int. J. Radiat. Biol. 1996; 69: 739-755.

10. Hawkins RB. A microdosimetric-kinetic model for the effect of non-Poisson distribution of lethal lesions on the variation of RBE with LET. Radiat. Res. 2003; 160: 61-90.

11. Cunha M, Monini C, Testa E, Beuve M. NanOx: A new theoretical framework for predicting radiation effectiveness in the context of particle therapy. Phys. Med. Biol. 2017; 62:1248-1268.

12. Monini C, Testa E, Beuve M. NanOx predictions of cell survival probabilities for three cell lines. Acta Phys. Pol. B 2017; 48: 1653-1660.

13. Monini C, Cunha M, Testa E, Beuve M. Study on the influence of NanOx parameters. Cancers 2018;10: E87.

14. Beuve M. Formalization and theoretical analysis of the LEM. Radiat. Res. 2009; 172: 394-402.

15. Katz R, Ackerson B, Homayoonfar M, Sharma SC. Inactivation of cells by heavy ion bombardment. J. Radiat. Res. 1971; 47: 402-425.

16. Russo G, Peroni C. Development of a radiobiological database for carbon ion treatment planning systems. PhD Thesis 2011; Università di Torino.

17. Friedrich T, Scholz U, Elsässer T, Durante M, Scholz M. Systematic analysis of RBE and related quantities using a database of cell survival experiments with ion beam irradiation. J. Radiat. Res. 2012; 54: 494-514.

18. Stewart RD, Carlson DJ, Butkus MP, Hawkins R, Friedrich T, Scholz M. A comparison of mechanism-inspired models for particle relative biological effectiveness (RBE). Med. Phys. 2018; 45: e926

19. Kase Y, T. Kanai T, Y. Furusawa Y, Okamoto H, Asaba T, Sakama M et al. Microdosimetric measurements and estimation of human cell survival for heavy-ion beams. Radiat. Res. 2006; 166: 629-638.

20. Kase Y, Kanai T, Matsufuji N, Furusawa Y, Elsasser T, Scholz M. Biophysical calculation of cell survival probabilities using amorphous track structure models for heavy-ion irradiation. Phys. Med. Biol. 2008; 53: 37-59.

21. Inaniwa T, Furukawa T, Kase Y, Matsufuji N, Toshito T, Matsumoto Y et al. Treatment planning for a scanned carbon beam with a modified microdosimetric kinetic model. Phys. Med. Biol. 2010; 55: 6721–6737.

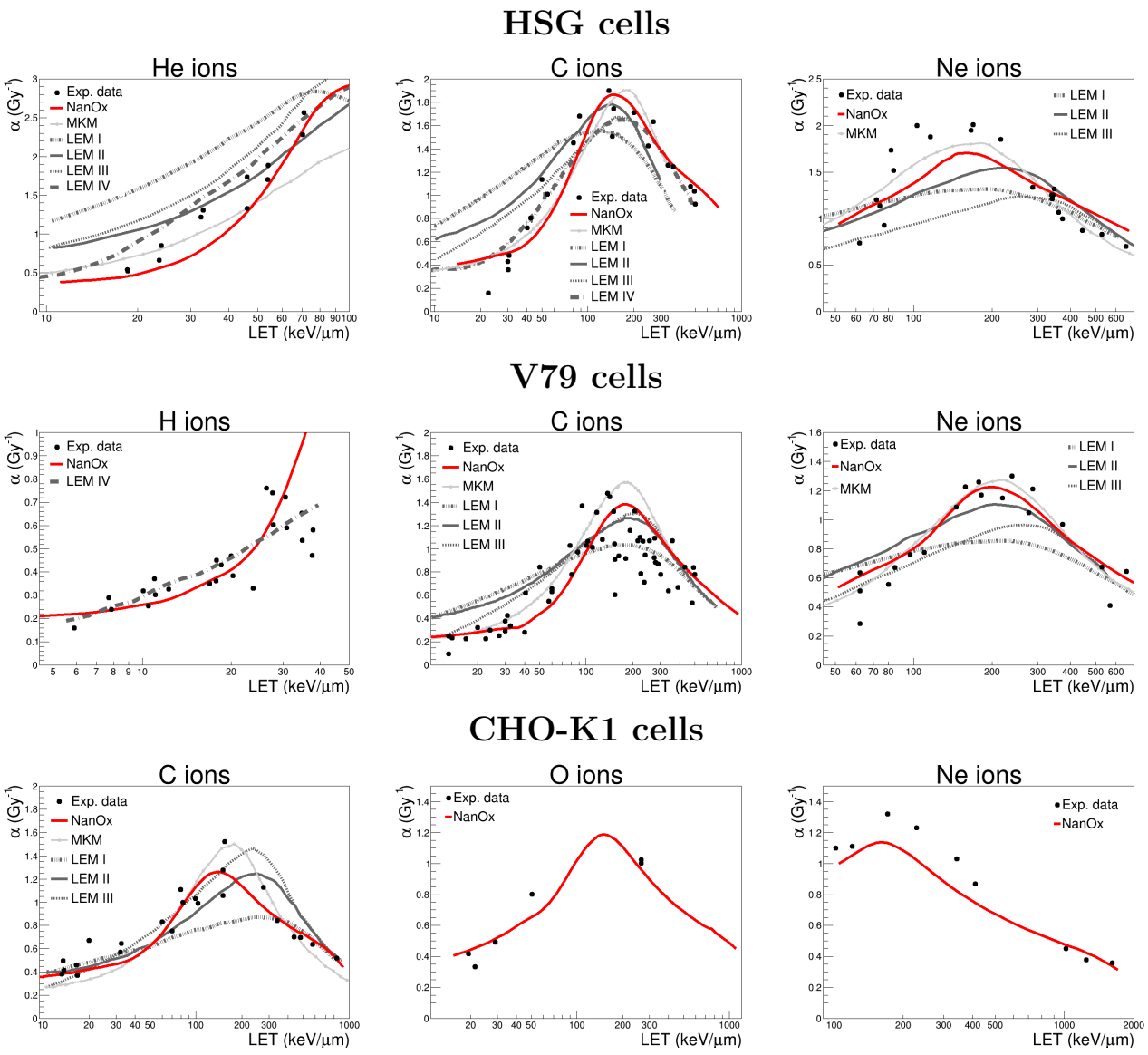

Figure 1: Evolution of the slope α with LET for HSG, V79 and CHO-K1 cells irradiated by hydrogen, helium, carbon, oxygen and neon ions. The experimental values gathered from the PIDE database [17] are compared with the predictions provided by the four versions of the LEM (when available), the MKM and NanOx. The data relative to the LEM and the MKM are extracted from [8, 16]. All the models are evaluated considering a single set of parameters for each cell line, which have been chosen as they optimize the agreement with the experimental points.

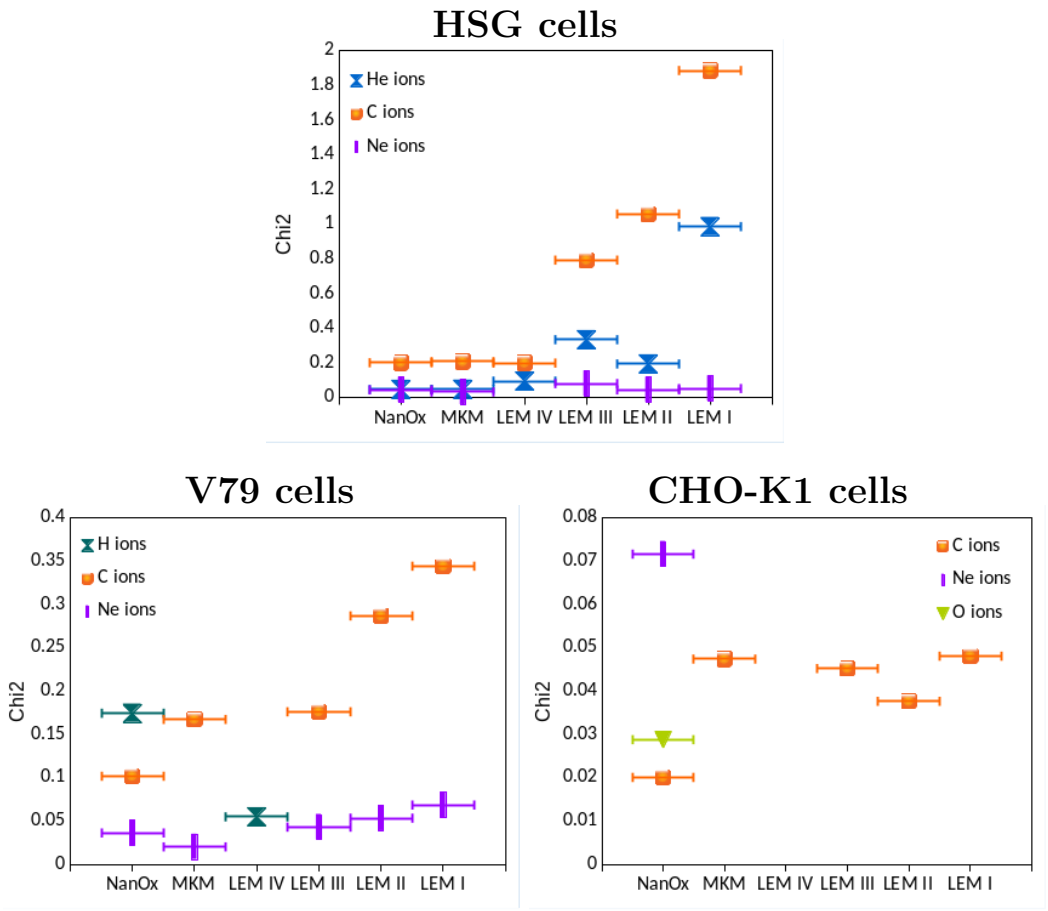

Figure 2: χ^2 associated to each radiobiological model on the basis of the experimental and predicted points of Figure 1. The symbols represent the values computed separately for HSG, V79 and CHO-K1 cells irradiated by hydrogen, helium, carbon and neon ions. The solid lines, instead, are for visual guidance purposes only.

Cell line	**Model parameters**			
	LEM (I/II/III)	**LEM IV**	**MKM**	**NanOx**
HSG	α_x=0.313 Gy^{-1} β_x=0.062 Gy^{-2} D_t=30/6/19 Gy R_N=5 μm	α_x=0.316 Gy^{-1} β_x=0.062 Gy^{-2} D_t=7.5 Gy R_N=5 μm	α_0=0.313 Gy^{-1} β=0.062 Gy^{-2} R_d=0.02 μm R_n=4.6 μm	z_0=15654 Gy σ=549 Gy h=179439 β_G=0.096 Gy^{-2} R_{SV}=7 μm
V79	α_x=0.184 Gy^{-1} β_x=0.020 Gy^{-2} D_t=70/15/60 Gy R_N=4.2 μm	α_x=0.129 Gy^{-1} β_x=0.049 Gy^{-2} D_t=3 Gy R_N=5 μm	α_0=0.184 Gy^{-1} β=0.020 Gy^{-2} R_d=0.1 μm R_n=4.2 μm	z_0=22789 Gy σ=8117 Gy h=225841 β_G=0.041 Gy^{-2} R_{SV}=4.9 μm
CHO-K1	α_x=0.228 Gy^{-1} β_x=0.020 Gy^{-2} D_t=40/9.5/55 Gy R_N=4.7 μm		α_0=0.228 Gy^{-1} β=0.020 Gy^{-2} R_d=0.12 μm R_n=4.0 μm	z_0=14507 Gy σ=2781 Gy h=104810 β_G=0.063 Gy^{-2} R_{SV}=5.9 μm

Table 1: Values of the LEM (I-IV), MKM and NanOx parameters with which the predicted $\alpha(LET)$ curves of Figure 1 have been obtained. The set of parameters of each model was determined to optimize the agreement with the experimental data, as reported in [8, 13, 16].

Irradiation configuration	**Model:**					
	LEM I	**LEM II**	**LEM III**	**LEM IV**	**MKM**	**NanOx**
HSG, He ions	0.988	0.195	0.335	0.097	0.050	0.048
HSG, C ions	1.887	1.060	0.794	0.201	0.209	0.202
HSG, Ne ions	0.054	0.046	0.082	-	0.034	0.046
V79, H ions	-	-	-	0.055	-	0.175
V79, C ions	0.344	0.287	0.176	-	0.167	0.102
V79, Ne ions	0.069	0.054	0.043	-	0.020	0.036
CHO-K1, C ions	0.048	0.038	0.045	-	0.047	0.020
CHO-K1, Ne ions	-	-	-	-	-	0.380
CHO-K1, O ions	-	-	-	-	-	0.076

Table 2: Values of the χ^2 estimator for all the models and irradiation configurations presented in Fig.2